Nuclear Medicine and Biology 90–91 (2020) 49–54

Contents lists available at ScienceDirect

Nuclear Medicine and Biology

journal homepage: www.elsevier.com/locate/nucmedbio

[^{131}I]MIBG exports via MRP transporters and inhibition of the MRP transporters improves accumulation of [^{131}I]MIBG in neuroblastoma

Masato Kobayashi [a,*], Asuka Mizutani [a], Kodai Nishi [b], Yuka Muranaka [c], Ryuichi Nishii [d], Naoto Shikano [e], Takeo Nakanishi [f], Ikumi Tamai [g], Eugenie S. Kleinerman [h], Keiichi Kawai [a,i]

[a] School of Health Sciences, Institute of Medical, Pharmaceutical and Health Sciences, Kanazawa University, Kanazawa, Japan
[b] Department of Radioisotope Medicine, Atomic Bomb Disease Institute, Nagasaki University, Nagasaki, Japan
[c] Division of Health Sciences, Graduate School of Medical Sciences, Kanazawa University, Kanazawa, Japan
[d] Department of Molecular Imaging and Theranostics, National Institute of Radiological Sciences, National Institutes for Quantum and Radiological Science and Technology, Chiba, Japan
[e] Department of Radiological Sciences, Ibaraki Prefectural University of Health Sciences, Ibaraki, Japan
[f] Faculty of Pharmacy, Takasaki University of Health and Welfare, Takasaki, Japan
[g] School of Pharmaceutical Sciences, Institute of Medical, Pharmaceutical and Health Sciences, Kanazawa University, Kanazawa, Japan
[h] Division of Pediatrics, University of Texas M.D. Anderson Cancer Center, Houston, USA
[i] Biomedical Imaging Research Center, University of Fukui, Fukui, Japan

ARTICLE INFO

Article history:
Received 27 June 2020
Received in revised form 12 September 2020
Accepted 22 September 2020
Available online xxxx

Keywords:
[$^{123/131}$I]MIBG
Neuroblastoma
Efflux transporter
MRP
Probenecid

ABSTRACT

Introduction: ^{131}I-labeled *m*-iodobenzylguanidine ([^{131}I]MIBG) has been used to treat neuroblastoma patients, but [^{131}I]MIBG may be immediately excreted from the cancer cells by the adenosine triphosphate binding cassette transporters, similar to anticancer drugs. The purpose of this study was to clarify the efflux mechanism of [^{131}I]MIBG in neuroblastomas and improve accumulation by inhibition of the transporter in neuroblastomas.
Methods: [^{131}I]MIBG was incubated in human embryonic kidney (HEK)293 cells expressing human organic anion transporting polypeptide (OATP)1B1, OATP1B3, OATP2B1, organic anion transporter (OAT)1 and OAT2, organic cation transporter (OCT)1 and OCT2, and sodium taurocholate cotransporting polypeptide, and in vesicles expressing P-glycoprotein (MDR1), multidrug resistance associated protein (MRP)1–4, or breast cancer resistance protein with and without MK-571 and probenecid (MRP inhibitors). Time activity curves of [^{131}I]MIBG with and without MK-571 and probenecid were established using an SK-N-SH neuroblastoma cell line, and transporter expression of multiple drug resistance was measured. Biodistribution and SPECT imaging examinations were conducted using [^{123}I]MIBG with and without probenecid in SK-N-SH-bearing mice.
Results: [^{131}I]MIBG uptake was significantly higher in OAT1, OAT2, OCT1, and OCT2 than in mock cells. Uptake via OCT1 and OCT2 was little inhibited by MK-571 and probenecid. [^{131}I]MIBG uptake into vesicles that highly expressed MRP1 or MRP4 was significantly higher in ATP than in AMP, and these inhibitors restored uptake to levels similar to that in AMP. Examining the time activity curves for [^{131}I]MIBG in SK-N-SH cells, higher expressions of MDR1, MRP1, MRP4, and MK-571, or probenecid loading produced significantly higher uptake than in control at most incubation times. The ratios of tumors to blood or muscle in SK-N-SH-bearing mice were significantly increased by probenecid loading in comparison with normal mice.
Conclusions: [^{131}I]MIBG exports via MRP1 and MRP4 in neuroblastoma. The accumulation and tumor-to-blood or muscle ratios of [^{131}I]MIBG are improved by inhibition of MRPs with probenecid in neuroblastoma.
Advances in knowledge: [^{131}I]MIBG, widely used for treatment of neuroendocrine tumors including neuroblastoma, is excreted via MRP1 and MRP4 in neuroblastoma.
Implications for patient care: Loading with probenecid, OAT, and MRP inhibitors improves [^{131}I]MIBG accumulation.

1. Introduction

Neuroblastoma, which is derived from the neural crest, is the most common extracranial solid cancer in children [1]. Patients with metastatic neuroblastoma usually have a poor prognosis. To improve their poor prognosis, the accurate identification of all lesions is crucial to evaluate the extent of the neuroblastoma [2].

Iodine-123 labeled *m*-iodobenzylguanidine ([^{123}I]MIBG) and [^{131}I]MIBG, an analog of the adrenergic neurotransmitter norepinephrine, have been used as adrenomedullary scintigraphic agents with their gamma-rays since the early 1980s [3–5] and for detecting neuroendocrine tumors such as neuroblastoma, pheochromocytoma, and medullary thyroid cancer [6]. At present, [^{123}I]MIBG is routinely used for

* Corresponding author at: School of Health Sciences, Institutes of Medical, Pharmaceutical and Health Sciences, Kanazawa University, 5-11-80 Kodatsuno, Kanazawa 920-0942, Japan.
E-mail address: kobayasi@mhs.mp.kanazawa-u.ac.jp (M. Kobayashi).

https://doi.org/10.1016/j.nucmedbio.2020.09.004
0969-8051/

staging and follow-up of patients with neuroendocrine tumors and is suitable for [^{131}I]MIBG therapy. Because it emits beta rays with cytocidal effects, [^{131}I]MIBG has been used for the treatment of neuroendocrine tumors including neuroblastoma as a primary agent and in combination with other therapies [7,8].

In human cancers, organic anion transporting polypeptide (OATP) 1B1 (*SLCO1B1*), OATP1B3 (*SLCO1B3*), OATP2B1 (*SLCO2B1*), organic anion transporter (OAT)1 (*SLC22A6*), OAT2 (*SLC22A7*), organic cation transporter (OCT)1 (*SLC22A1*), OCT2 (*SLC22A2*), Na^+-taurocholate cotransporting polypeptide (NTCP) (*SLC10A1*) isoforms are expressed as solute carrier (SLC) transporters [9,10]. Many anticancer drugs and medicines are incorporated into tumors via these SLC transporters for cancer treatment.

When multiple drug resistance (MDR) with ATP-binding cassette (ABC) transporters occurs in cancer cells, anticancer drugs accumulate in the cancer cells and are then immediately excreted from the cancer cells [11,12]. Thus, the total amount of the anticancer drug decreases in the cancer cells, and the therapeutic effect decreases. The ABC transporters are classified into seven subfamilies based on phylogenetic analysis. In tumor cells, ABC proteins mainly include P-glycoprotein (P-gp and MDR1, gene symbol *ABCB1*), multidrug resistance protein 1 (MRP1, gene symbol *ABCC1*), MRP2 (gene symbol *ABCC2*), MRP3 (gene symbol *ABCC3*), MRP4 (gene symbol *ABCC4*), and breast cancer resistance protein (BCRP, gene symbol *ABCG2*).

Since the effect of internal radiotherapy with [^{131}I]MIBG is not the same in all patients, there is uptake of [^{131}I]MIBG into the cancer cells once, and it may be immediately excreted from the cancer cells by the ABC transporters, as in the case of anticancer drugs. Thus, the therapeutic effect of [^{131}I]MIBG may change in every patient based on the total amount of [^{131}I]MIBG accumulated in tumor cells. If the injected radioactivity of [^{131}I]MIBG was increased, uptake of [^{131}I]MIBG into neuroblastoma may be improved, but whole-body radiation exposure would be higher. An alternative strategy is needed to improve [^{131}I]MIBG accumulation in tumor cells.

Although it has been reported that P-gp is not involved in efflux of [^{131}I]MIBG [13], the relationship between [^{131}I]MIBG and other ABC transporters has not been evaluated. The purpose of this study was to elucidate the efflux mechanism of [^{131}I]MIBG in neuroblastomas and improve accumulation by inhibition of the transporters in neuroblastomas.

2. Material and methods

2.1. Materials

[^{123}I]MIBG (74 MBq/mL, more than 95% purity) for biological distribution and single photon emission computed tomography (SPECT) imaging, instead of [^{131}I]MIBG and [^{131}I]MIBG (370 MBq/mL), was purchased from FUJIFILM Toyama Chemical Co., Ltd. (Tokyo, Japan) and IZOTOP Institute of Isotopes Co., Ltd. (Budapest, Hungary), respectively. MK-571 sodium salt and probenecid were purchased from Cayman Chemical (Ann Arbor, MI, USA) and Sigma-Aldrich (St. Louis, MO, USA), respectively.

2.2. Human embryonic kidney (HEK)293 cells for SLC transporters and vesicles for ABC transporters

As SLC transporters, HEK293 cells expressing OATP1B1, OATP1B3, OATP2B1, OAT1, OAT2, OCT1, OCT2, and NTCP plasmid vector alone for mock cells were prepared as described previously [14]. Briefly, HEK293 cells were transfected with the respective plasmid DNA, and they were then selected with the appropriate antibiotics; HEK293/OATP1B1, HEK293/OATP1B3, HEK293/OATP2B1, HEK293/OAT1, HEK293/OAT2, HEK293/OCT1 HEK293/OCT2, and HEK293/NTCP cells and mock cells were designed. All cell lines were grown in Dulbecco's modified eagle medium (Wako Pure Chemical Industries Ltd., Osaka, Japan) supplemented with 10% (v/v) fetal bovine serum (Life Technologies, Carlsbad, CA), 100 U/mL penicillin, and 100 μg/mL streptomycin at 37 °C and 5% CO_2.

As ABC transporters, vesicles (GenoMembrane Inc., Kanagawa, Japan) with high expression of human MDR1, MRP1–4, and BCRP were used. Experimental kits were also purchased from GenoMenbrane Inc. and used for experiments with each ABC transporter.

2.3. Uptake experiments with HEK293 cells

First, expression levels of SLC transporters were confirmed in the HEK293 cells expressing OATP using [6,7-^{3}H(N)]estrone-3-sulfate (PerkinElmer Inc., Waltham, MA, USA, 2.04 GBq/mmol, 2.22 TBq/mmol), OAT using *p*-[^{14}C]aminohippuric acid (PerkinElmer Inc., 2.04 GBq/mmol), OCT using [^{3}H]methyl-4-phenylpyridinium (American Radiolabeled Chemicals Inc., St. Louis, MO, USA, 2.96 TBq/mmol), and NTCP using [^{3}H(G)]taurocholic acid (PerkinElmer Inc., 37 GBq/mmol). One day before the uptake experiments, HEK293 cells expressing an SLC transporter were prepared at 4×10^5 cells/well in 12-well plastic plates. Cells were pre-incubated for 10 min using modified Hank's balanced salt solution. Each cell was incubated with [^{131}I]MIBG (37 kBq) for 5 min ($n = 4$) and removed from the tissue culture by 0.25% trypsin-EDTA solution (Sigma-Aldrich). Then, the radioactivity of the cells was measured using a gamma counter. For protein assays of the cells, cellular protein content was measured with a BCA protein assay kit (Thermo Fisher Scientific Inc., Waltham, MA, USA) using BSA as a standard. Uptakes of [^{131}I]MIBG in HEK293/OATP1B1, HEK293/OATP1B3, HEK293/OATP2B1, HEK293/OAT1, HEK293/OAT2, HEK293/OCT1, HEK293/OCT2, and HEK293/NTCP were compared with that in mock HEK293 cells. Using assays with inhibitors, uptake of [^{131}I]MIBG was examined in HEK293/OAT1, HEK293/OAT2, HEK293/OCT1, and HEK293/OCT2 cells with MK-571, a substrate for OATs [15] and an MRP inhibitor [16,17], and probenecid, a substrate for OATs [18], OCTs [19], and MRP inhibitors [16,17]. The uptake of [^{131}I]MIBG is shown as % injected dose (%ID)/mg protein.

2.4. Uptake experiments with vesicles

After pre-incubation of vesicles for 10 min using reaction buffer including 50 mM MOPS-Tris, 70 mM KCl, and 7.5 mM $MgCl_2$ in the kit, 37 kBq [^{131}I]MIBG were incubated for 5 min with each vesicle solution and ATP ($n = 4$), which supplies energy for ABC transporters, or adenosine monophosphate (AMP, $n = 4$), which does not provide energy and was used for comparison to ATP, on nitrocellulose filters, and radioactivity was measured using a γ-ray counter (AccuFLEXγ7000, Aloka, Tokyo, Japan). Uptake of [^{131}I]MIBG in ATP solution was compared with that in AMP solution. When uptake of [^{131}I]MIBG in ATP solution was higher than that in AMP solution, this indicated an effect of ^{131}I-MIBG on ABC transporters. In assays with inhibitors, uptake of [^{131}I]MIBG was examined in ATP solution with MK-571 and probenecid (MRP inhibitors) using vesicle solution with high expressions of MRP1 and MRP4. The uptake of [^{131}I]MIBG is shown as nmol/mg protein.

2.5. SK-N-SH neuroblastoma cell line

The cultured human cancer cell line SK-N-SH neuroblastoma was purchased from American Type Culture Collection (Manassas, VA, USA). Cancer cells were incubated in αMEM (Wako, Osaka, Japan) with 10% fetal bovine serum.

2.6. Expression of ABC transporters in SK-N-SH cells using real-time PCR

Expression of ABC transporters in human cancer cells was evaluated as described [19]. The following genes were analyzed using real-time polymerase chain reaction with an Mx3005P thermocycler (Agilent Technologies, Santa Clara, CA, USA): MDR1 (*ABCB1*) and MRP1, 2, 3, and 4 (*ABCC1*, *2*, *3* and *4*) and BCRP (*ABCG2*). Three different housekeeping genes, glyceraldehyde-3-phosphate dehydrogenase (GAPDH), beta actin (ACTB), and hypoxanthine phosphoribosyltransferase-1 (HPRT1),

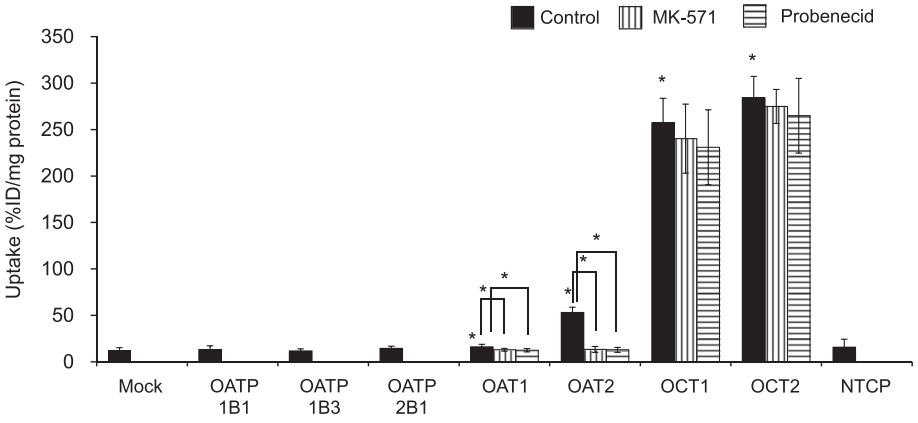

Fig. 1. Uptake of [^{131}I]MIBG by HEK293 cells expressing an SLC transporter (n = 4). [131I]MIBG uptake is significantly higher in HEK293/OAT1, HEK293/OAT2, HEK293/OCT1, and HEK293/OCT2 cells than in mock cells. Although the uptake of HEK293/OAT1 and HEK293/OAT2 cells is significantly inhibited by MK-571 and probenecid, the uptake of HEK293/OCT1 and HEK293/OCT2 cells is little inhibited. *$P < 0.05$ vs. mock cells, between control of HEK293 cells and HEK293 with MK-571 or probenecid loading.

were amplified to control for the differences between the initial RNA and cDNA amounts.

2.7. Transport assays with SK-N-SH

Transport assays were performed as described [20]. One day after seeding of SK-N-SH cells, each well was pre-incubated with 1 mL of incubation medium for 10 min. The cells were then incubated with 37 kBq [^{131}I]MIBG for 1, 3, 5, 10, 30, 60, 120, or 180 min at 37 °C (n = 4). For the competitive inhibition assay, the cells were incubated for the above incubation time with [^{131}I]MIBG in the presence of inhibitor: final concentration 50 μM MK-571 sodium salt [16,17] or 1 mM probenecid for MRP1–4 [16,17]. At the end of the incubation, each well was rapidly washed twice with 1 mL of ice-cold incubation medium. The cells were then solubilized in 0.5 mL 0.1 N NaOH, and radioactivity was measured with a γ-ray counter. The uptake of [^{131}I]MIBG is shown as nmol/mg protein.

2.8. Biological distribution of [^{123}I]MIBG in SK-N-SH-bearing mice

All applicable institutional guidelines for the care and use of animals were followed at Kanazawa University. All procedures performed in studies involving animals were in accordance with the ethical standards of Kanazawa University (the Animal Care Committee of Kanazawa University, AP-122339) and were conducted in accordance with the international standards for animal welfare and institutional guidelines. Twenty-four Scid mice (female, 5 weeks old, SLC Inc., Hamamatsu, Japan) were transplanted with SK-N-SH cells (5×10^5 cells/100 μL) and Matrigel (#354230, Corning, Corning, NY, USA) into the lower abdomen of the mice. The mice were housed for about 5–7 weeks under a 12-h light/12-h dark cycle with free access to food and water. The mice were fasted with no food overnight with water supplied ad libitum before experiments. About 1 month later, the size of the SK-N-SH tumor became palpable with a diameter of 5–10 mm. Then, 200 kBq [^{123}I]MIBG were injected via the tail vein in SK-N-SH-bearing mice. Mice were sacrificed at 10, 30, 60, and 120 min post-injection (each n = 3). After blood was sampled via cardiocentesis, brain, heart, liver, kidney, muscle, and the SK-N-SH tumor were excised. Radioactivity in weighed tissue samples was measured using a gamma counter (ARC-380; Aloka). Data are expressed as injected dose per g wet tissue (%ID/g tissue). For the loading study of probenecid, which has a high safety level for humans, the SK-N-SH-bearing mice were injected with a mixture of [^{123}I]MIBG and 1 mM probenecid, and the distribution studies were performed using the same protocol that was used for SK-N-SH-bearing mice without probenecid loading as control mice.

2.9. SPECT imaging with [^{123}I]MIBG in SK-N-SH-bearing mice

[^{123}I]MIBG (30–40 MBq, n = 3) or a mixture of [^{123}I]MIBG and 1 mM probenecid (n = 3) were injected into the tail vein of SK-N-SH-bearing mice, SPECT acquisition was started 5 min after injection, and SPECT im-

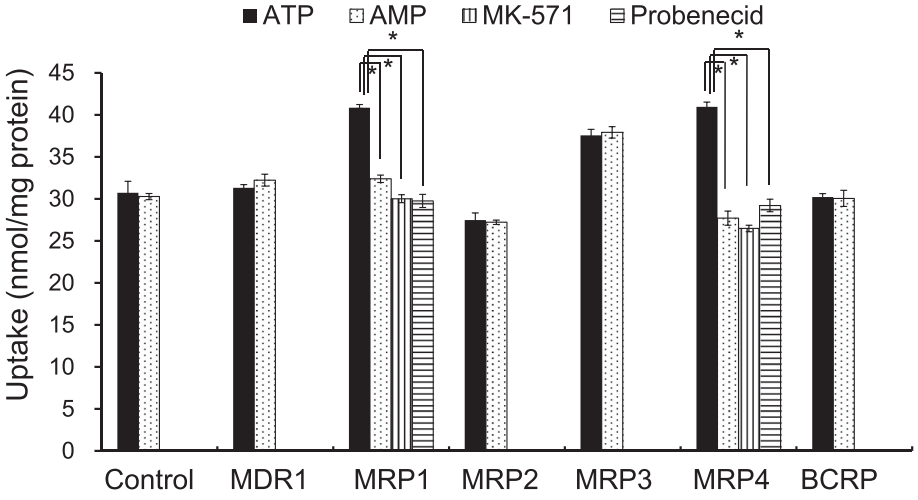

Fig. 2. Uptake of [^{131}I]MIBG by vesicles overexpressing each ABC transporter (n = 4). [131I]MIBG uptake into vesicles that highly expressed MRP1 or MRP4 in the presence of ATP is significantly higher than that in the presence of AMP, but not MDR1, MRP2, MRP3, and BCRP. Uptake via MRP4 is higher than that via MRP1. In MK-571 or probenecid loading, uptake of [^{131}I]MIBG decreases to levels similar to that in AMP solution. *$P < 0.05$ vs. presence of AMP, ATP with MK-571 or probenecid loading.

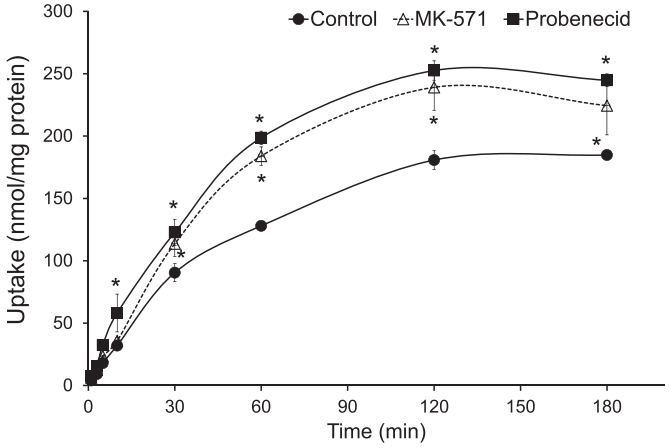

Fig. 3. Time activity curves for [^{131}I]MIBG in SK-N-SH cells (n = 4). MK-571 or probenecid loading produces significantly higher uptake than in normal mice at most incubation times. At 120 min of incubation, uptake of [^{131}]MIBG and MK-571 loading is about 1.4-fold higher than in the control, and that with probenecid loading is about 1.5-fold higher. However, there is no significant difference between MK-571 loading and probenecid loading. * $P < 0.05$ vs. control.

ages were obtained at 10–15 min and 60–65 min using a U-SPECT-II/CT system (MILabs, Utrecht, The Netherlands). The data were reconstructed using the ordered subset expectation maximization method with 16 subsets and six iterations, including no scatter and attenuation correction. The voxel size was set to 0.8 × 0.8 × 0.8 mm^3. Post-reconstruction smoothing filtering was applied using a 1.0-mm Gaussian filter. Image displays were obtained and analyzed using medical image data analysis software, AMIDE (ver. 1.0.4). Coronal images are displayed as similar section images.

2.10. Statistical analysis

Data are presented as means and standard deviation (SD). *P* values were calculated using the two-tailed paired Student's *t*-test for comparison between two groups or analysis of variance and Dunnett's test, which were used as a multiplex analysis with a population mean value, using GraphPad Prism 7 statistical software (GraphPad Software, Inc., La Jolla, CA, USA). A *P* value less than 0.01 or 0.05 was considered significant.

3. Results

Fig. 1 shows uptake of [^{131}I]MIBG by HEK293 cells expressing an SLC transporter. [^{131}I]MIBG uptake was significantly higher in control of HEK293/OAT1, HEK293/OAT2, HEK293/OCT1, and HEK293/OCT2 cells than in mock cells. Although the uptake of HEK293/OAT1 and HEK293/OAT2 cells was significantly inhibited by MK-571 and probenecid, the uptake of [^{131}I]MIBG via HEK293/OCT1 and HEK293/OCT2 cells was little inhibited. Fig. 2 shows the uptake of [^{131}I]MIBG by vesicles overexpressing each ABC transporter. [^{131}I]MIBG uptake into vesicles that highly expressed MRP1 or MRP4 in the presence of ATP was significantly higher than that in the presence of AMP, but not MDR1, MRP2, MRP3, and BCRP. MK-571 or probenecid loading in vesicle solution with high expression of MRP1 or MRP4 in the presence of ATP solution restored uptake levels of [^{131}I]MIBG similar to that in AMP solution. After confirming the high quality of the total RNA harvested from SK-N-SH cells using a bioanalyzer (data not shown), genes for transporters of MDR1 (25.83 as the copy number per 1000 copies of housekeeping genes), MRP1 (23.41), and MRP4 (6.76) were highly expressed in comparison with MRP2 (0.16), MRP3 (0.75), and BCRP (0.00). In the time activity curves of [^{131}I]MIBG in SK-N-SH cells (Fig. 3), MK-571 or probenecid loading produced significantly higher uptake than in the control at most incubation times. At 120 min of incubation, uptake of [^{131}]MIBG with MK-571 loading was about 1.4-fold higher than in the control, and that with probenecid loading was about 1.5-fold higher. However, there was no significant difference between MK-571 loading and probenecid loading.

The biological distribution (Table 1) and SPECT images (Fig. 4) of SK-N-SH-bearing mice injected using [^{123}I]MIBG with or without probenecid loading were obtained. With respect to the biological distribution of [^{123}I]MIBG, [^{123}I]MIBG accumulated mainly in blood, heart, liver, kidney, and SK-N-SH tumors. [^{123}I]MIBG injection with probenecid loading resulted in high accumulation in heart, liver, kidney, and SK-N-SH tumors at 30 min and/or 60 min after administration in comparison with normal mice. At 120 min after administration, accumulation in the heart and SK-N-SH tumors with probenecid loading increased significantly compared with normal mice. On SPECT images at 10–15 min after [^{123}I]MIBG with and without probenecid loading, radioactivity (%ID/g mice weight) of [^{123}I]MIBG was 4.8 ± 3.1 and 3.8 ± 2.9 in heart, 5.1 ± 1.7 and 3.3 ± 1.8 in liver, 3.0 ± 1.3 and 2.6 ± 1.1 in kidney and 1.5 ± 0.5 and 1.0 ± 0.4 in SK-N-SH tumors with and without probenecid loading, respectively. At 60–65 min after [^{123}I]MIBG with and without probenecid loading, 4.9 ± 0.8 and 3.4 ± 0.8 in heart, 5.7 ± 1.2 and 4.3 ± 1.1 in liver, 1.7 ± 0.5 and 1.2 ± 0.3 in kidney and 1.4 ± 0.4 and 0.8 ± 0.2 in SK-N-SH tumors, respectively.

4. Discussion

In this study, the efflux mechanism of [^{131}I]MIBG was clarified, and the accumulation of [^{131}I]MIBG in neuroblastoma was improved. The influx

Table 1
Biological distribution of [^{123}I]MIBG in mice with and without probenecid loading.

	Organ (%ID/g)	10 min	30 min	60 min	120 min
Normal mice	Blood	1.90 ± 0.45	1.66 ± 0.65	1.42 ± 0.12	1.33 ± 0.11
	Brain	0.30 ± 0.06	0.20 ± 0.08	0.19 ± 0.08	0.17 ± 0.07
	Heart	28.98 ± 1.72	23.14 ± 2.03	19.47 ± 1.95	16.65 ± 1.89
	Liver	12.85 ± 3.18	23.97 ± 4.53	18.65 ± 3.83	16.11 ± 3.46
	Kidney	9.13 ± 1.85	8.07 ± 1.69	6.42 ± 1.73	3.89 ± 1.59
	Muscle	1.82 ± 0.49	1.55 ± 0.48	1.48 ± 0.42	1.38 ± 0.39
	Tumor	3.12 ± 0.83	2.53 ± 0.72	2.01 ± 0.63	1.84 ± 0.60
Probenecid loading	Blood	1.98 ± 0.32	1.70 ± 0.59	1.43 ± 0.18	1.34 ± 0.13
	Brain	0.20 ± 0.05	0.15 ± 0.06	0.14 ± 0.08	0.14 ± 0.06
	Heart	29.65 ± 0.91	25.82 ± 0.93*	21.02 ± 1.05*	18.94 ± 1.32*
	Liver	13.12 ± 4.02	28.31 ± 6.83*	20.13 ± 4.58*	17.12 ± 2.74
	Kidney	10.21 ± 1.67	9.52 ± 1.44*	7.82 ± 1.45*	3.94 ± 1.59
	Muscle	1.80 ± 0.26	1.58 ± 0.32	1.35 ± 0.26	1.28 ± 0.36
	Tumor	3.34 ± 0.83	2.78 ± 0.81	2.38 ± 0.71*	2.17 ± 0.69*

%ID/g indicates percent injected dose per gram of tissue. Values are the means ± standard deviation obtained from three mice.
* $P < 0.05$ compared with normal mice.

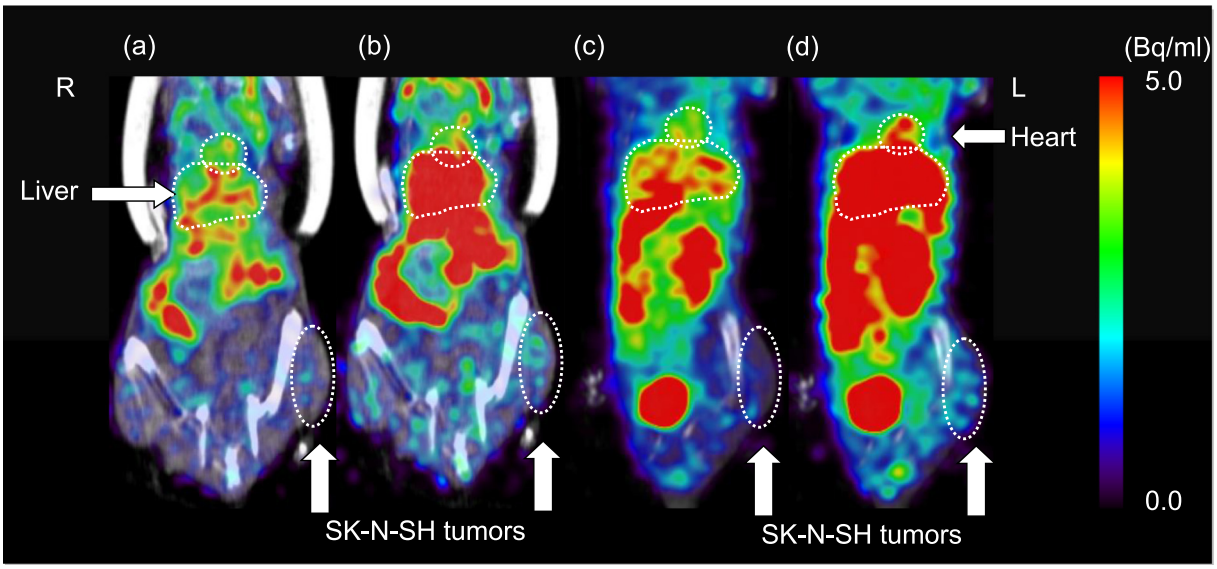

Fig. 4. Representative [^{123}I]MIBG SPECT imaging without (a, c) and with probenecid loading (b, d) at 10–15 min (a, b) and 60–65 min (c, d) after administration.

mechanism of [^{131}I]MIBG was investigated to improve the accumulation of [^{131}I]MIBG using inhibitors of efflux transporters in neuroblastoma. Bayer has reported that [^{131}I]MIBG uptake into neuroblastoma occurs via OCT3, for which another name is norepinephrine transporter, [20], and the present results showed that [^{131}I]MIBG uptake involves OCT1 and OCT2 (Table 1). Anion drugs are usually transported by OATs, which are SLC transporters, and MRPs in the cells [21]. Although uptake of [^{131}I]MIBG was inhibited by MK-571 and probenecid in HEK293/OAT1 and HEKOAT2 cells (Fig. 1) because MK-571 [15] and probenecid [18,22] are mainly transported by OATs, uptake of [^{131}I]MIBG was little inhibited by MK-571 and probenecid in HEK293/OCT1 and HEK293/OCT2 cells (Fig. 1). In assays with vesicles (Fig. 2), [^{131}I]MIBG uptake into vesicles with high expression of MRP1 or MRP4 was significantly higher in ATP solution than in AMP solution, but not with MDR1, MRP2, MRP3, and BCRP. Therefore, MK-571 or probenecid was loaded in MRP1 or MRP4 in ATP solution, and similar uptake levels of [^{131}I]MIBG to that in AMP solution were obtained. In the SK-N-SH cells (Fig. 3) and examining gene expression in SK-N-SH cells, [^{131}I]MIBG effluxed via MRP1 and MRP4 in neuroblastomas. [^{131}]MIBG with MK-571 or probenecid loading was given to SK-N-SH cells, efflux of [^{131}I]MIBG was inhibited by MK-571 or probenecid, and then the accumulation of [^{131}I]MIBG was significantly increased in SK-N-SH cells (Fig. 3). The increase rate was slightly higher with probenecid than with MK-571. Since probenecid has higher safety and easier clinical application for human use than MK-571 [16,23], improvement of the effect of internal radiation therapy in neuroblastoma using co-injection of [^{131}I]MIBG and probenecid was evaluated.

With respect to the biological distribution in SK-N-SH-bearing mice with probenecid loading (Table 1), [^{123}I]MIBG with probenecid loading provided significantly higher accumulation in heart, liver, kidney, and SK-N-SH tumors at 30 min and/or 60 min after administration compared with in normal mice. Since MRP1 and/or MRP4, which are involved in efflux of [^{131}I]MIBG, are expressed in heart, liver, and kidney [12] and the SK-N-SH tumors that were evaluated, the accumulation of [^{123}I]MIBG was increased 1.18 and 1.18 times at 60 min and 120 min, respectively, after [^{123}I]MIBG administration with probenecid loading through inhibition of [^{123}I]MIBG efflux via MRP1 and/or MRP4. It was found that, 120 min after administration of [^{123}I]MIBG with probenecid loading, washout of [^{123}I]MIBG in heart, liver, kidney and SK-N-SH tumors was slower than in normal mice. The effect of probenecid loading may be maintained due to the high biostability of [$^{123/131}$I]MIBG [24,25] and probenecid [16]. Therefore, slower washout of [^{131}I]MIBG in heart, liver and kidney may yield increase of radiation dose by the probenecid loading. The ratios of SK-N-SH tumors to blood and of SK-N-SH tumors to muscle were evaluated to examine image contrast in SPECT imaging. The ratio of SK-N-SH tumors to blood was significantly increased by probenecid loading in comparison with normal mice at 30 min, 60 min, and 120 min after administration, while the ratio of SK-N-SH tumors to muscle was significantly increased by probenecid loading in comparison with normal mice at all injection times (Table 2). The higher ratios of SK-N-SH tumors to blood or SK-N-SH tumors to muscle show higher contrast images between SK-N-SH tumors and backgrounds. On SPECT imaging using [^{123}I]MIBG with probenecid loading at 60–65 min after administration, accumulation of [^{123}I]MIBG was increased in heart, liver, kidney, and SK-N-SH tumors compared with normal mice (Fig. 4).

The potential to improve internal radiation therapy with [^{131}I]MIBG for neuroblastoma using a combination of [^{131}I]MIBG and MRP inhibitors should be demonstrated. Although probenecid shows high safety, it sometimes has common side effects, such as an allergic reaction, with high-dose loading. Additional experiments to determine Kaplan-Meier survival estimates, etc. with neuroblastoma-bearing mice are needed to evaluate improvement of internal radiation therapy with [^{131}I]MIBG.

5. Conclusion

[^{131}I]MIBG is exported via MRP1 and MRP4 in neuroblastoma. The accumulation and tumor-to-blood or muscle ratios of [^{131}I]MIBG

Table 2
Ratios of SK-N-SH tumors to blood and SK-N-SH tumors to muscle.

		10 min	30 min	60 min	120 min
Normal mice	Tumor to blood ratio	1.64 ± 0.51	1.52 ± 0.71	1.42 ± 0.61	1.38 ± 0.40
	Tumor to muscle ratio	1.71 ± 0.45	1.63 ± 0.55	1.36 ± 0.45	1.33 ± 0.42
Probenecid loading	Tumor to blood ratio	1.69 ± 0.55	1.64 ± 0.61*	1.66 ± 0.58*	1.62 ± 0.51*
	Tumor to muscle ratio	1.86 ± 0.49*	1.76 ± 0.58*	1.76 ± 0.50*	1.70 ± 0.48*

* $P < 0.05$ compared with normal mice.

improves with probenecid by inhibition of these transporters in neuroblastoma.

Financial support

This study was funded in part by Grants-in-Aid for Scientific Research from the Japan Society for the Promotion of Science (Nos. 15K09949, 15K15452, 16KK0200, 16H05397).

Author contributions

Masato Kobayashi was the research coordinator for the study.

Asuka Mizutani and Kodai Nishi performed biodistribution and SPECT imaging.

Ryuichi Nishi and Naoto Shikano were advisers for transport assays.

Takeo Nakanishi and Ikumi Tamai were advisors for vesicle assays.

Eugenie S. Kleinerman was an advisor for handling of neuroblastoma.

Keiichi Kawai was an advisor for handling of radiopharmaceuticals.

Acknowledgments

The authors would like to thank Mikie Ohtake and other staff of the School of Health Sciences, Kanazawa University.

Declaration of competing interest

There is no conflict of interest.

References

[1] Hoehner JC, Gestblom C, Hedborg F, Sandstedt B, Olsen L, Pahlman S. A developmental model of neuroblastoma: differentiating stroma-poor tumors' progress along an extra-adrenal chromaffin lineage. Lab Invest. 1996;75:659–75.
[2] Kinnier-Wilson LM, Draper GJ. Neuroblastoma, its natural history and prognosis: a study of 487 cases. Br Med J. 1974;3:301–7.
[3] Wieland DM, Wu JI, Brown LE. Radiolabeled adrenergic neuron-blocking agents: adrenomedullary imaging with [^{131}I]iodobenzylguanidine. J Nucl Med. 1980;21:349–53.
[4] Wieland DM, Brown LE, Tobes MC, Rogers WL, Marsh DD, Mangner, et al. Imaging the primate adrenal medulla with [^{123}I] and [^{131}I] meta-iodobenzylguanidine: concise communication. J Nucl Med. 1981;22:358–64.
[5] Nakajo M, Shapiro B, Copp J, Kalff V, Gross MD, Sisson JC, et al. The normal and abnormal distribution of the adrenomedullary imaging agent m-[I-131] iodobenzylguanidine (I-131 MIBG) in man: evaluation by scintigraphy. J Nucl Med. 1983;24:672–82.
[6] Bombardieri E, Giammarile F, Aktolun C, Baum RP, Delaloye AB, Maffioli L, et al. ^{131}I/^{123}I- Metaiodobenzylguanidine (mIBG) scintigraphy: procedure guidelines for tumour imaging. Eur J Nucl Med Mol Imaging. 2010;37:2436–46.
[7] Treuner J, Klingebiel T, Feine U, Buck J, Bruchelt G, Dopfer R, et al. Clinical experiences in the treatment of neuroblastoma with 131I-metaiodobenzylguanidine. Ped Hematol Oncol. 1986;3:205–16.
[8] Kayano D, Kinuya S. Iodine-131 metaiodobenzylguanidine therapy for neuroblastoma: reports so far and future perspective. Sci World J. 2015;2015:189135.
[9] Klaassen CD, Aleksunes LM. Xenobiotic, bile acid, and cholesterol transporters: function and regulation. Pharmacol Rev. 2010;62:1–96.
[10] Zollner G, Wagner M, Fickert P, Silbert D, Fuchsbichler A, Zatloukal K, et al. Hepatobiliary transporter expression in human hepatocellular carcinoma. Liver Int. 2005;25:367–79.
[11] Lockhart A, Tirona L, Kim R. Pharmacogenetics of ATP-binding cassette transporters in cancer and chemotherapy. Mol Cancer Ther. 2003;2:685–98.
[12] Nakanishi T. Drug transporters as targets for cancer chemotherapy. Cancer Genomics Proteomics. 2007;4:241–54.
[13] Kiyono Y, Yamashita T, Doi H, Kuge Y, Katsura T, Inui K, et al. Is MIBG a substrate of p-glycoprotein? Eur J Nucl Med Mol Imaging. 2007;34:448–52.
[14] Kobayashi M, Nakanishi T, Nishi K, Higaki Y, Okudaira H, Ono M, et al. Transport mechanisms of hepatic uptake and bile excretion in clinical hepatobiliary scintigraphy with ^{99m}Tc-*N*-pyridoxyl-5-methyltryptophan. Nucl Med Biol. 2014;41:338–42.
[15] Henjakovic M, Hagos Y, Krick W, Burckhardt G, Burckhardt BC. Human organic anion transporter 2 is distinct from organic anion transporters 1 and 3 with respect to transport function. Am J Physiol Renal Physiol. 2015;309:F843–51.
[16] Reid G, Wielinga P, Zelcer N, De Haas M, Van Deemter L, Wijnholds J, et al. Characterization of the transport of nucleoside analog drugs by the human multidrug resistance proteins MRP4 and MRP5. Mol Pharmacol. 2003;63:1094–103.
[17] Luna-Tortós C, Fedrowitz M, Löscher W. Evaluation of transport of common antiepileptic drugs by human multidrug resistance-associated proteins (MRP1, 2 and 5) that are overexpressed in pharmacoresistant epilepsy. Neuropharmacology. 2010;58:1019–32.
[18] Takahara N, Saga T, Inubushi M, Kusuhara H, Seki C, Ito S, et al. Drugs interacting with organic anion transporter-1 affect uptake of Tc-99m-mercaptoacetyltriglycine (MAG3) in the human kidney: therapeutic drug interaction in Tc-99m-MAG3 diagnosis of renal function and possible application of Tc-99m-MAG3 for drug development. Nucl Med Biol. 2013;40:643–50.
[19] Landersdorfer CB, Kirkpatrick CMJ, Kinzig M, Bulitta JB, Holzgrabe U, Jaehde U, et al. Competitive inhibition of renal tubular secretion of ciprofloxacin and metabolite by probenecid. Br J Clin Pharmacol. 2010;69:167–78.
[20] Bayer M, Schmitt J, Dittmann H, Handgretinger R, Bruchelt G, Sauter AW. Improved selectivity of mIBG uptake into neuroblastoma cells in vitro and in vivo by inhibition of organic cation transporter 3 uptake using clinically approved corticosteroids. Nucl Med Biol. 2016;43:543–51.
[21] Kobayashi M, Tsujiuchi T, Okui Y, Mizutani A, Nishi K, Nakanishi T, et al. Different efflux transporter affinity and metabolism of ^{99m}Tc-2-methoxyisobutylisonitrile and ^{99m}Tc-tetrofosmin for multidrug resistance monitoring in cancer. Pharm Res. 2018;36:18.
[22] Kobayashi M, Nishi K, Mizutani A, Okudaira H, Nakanishi T, Shikano N, et al. Transport mechanism and affinity of [^{99m}Tc]Tc-mercaptoacetyltriglycine ([^{99m}Tc]MAG3) on the apical membrane of renal proximal tubule cells. Nucl Med Biol. 2020;84-85:33–7.
[23] Beara-Lasic L, Pillinger MH, Goldfarb DS. Advances in the management of gout: critical appraisal of febuxostat in the control of hyperuricemia. Int J Nephrol Renovasc Dis. 2010;3:1–10.
[24] Mangner TJ, Tobes MC, Wieland DW, Sisson JC, Shapiro B. Metabolism of iodine-131 metaiodobenzylguanidine in patients with metastatic pheochromocytoma. J Nucl Med. 1986;27:37–44.
[25] Wafelman AR, Hoefnagel CA, Maes RA, Beijnen JH. A comparison of the radiochemical stability of different iodine-131 labelled metaiodobenzylguanidine formulations for therapeutic use. Appl Radiat. 1994;45:183–9.